Hydrogen bond dynamical properties of adsorbed liquid water monolayers with various TiO_2 interfaces

Niall J. English[1,2,a)], Ritwik S. Kavathekar[1] and J.M.D. MacElroy[1,2]

[1]The SFI Strategic Research Cluster in Solar Energy Conversion, School of Chemical and Bioprocess Engineering and [2]Centre for Synthesis and Chemical Biology University College Dublin, Belfield, Dublin 4, Ireland.

Keywords: Molecular Dynamics, Titania, Water, Hydrogen Bonds

Equilibrium classical molecular dynamics (MD) simulations have been performed to investigate the hydrogen bonding kinetics of water in contact with rutile-(110), rutile-(101), rutile-(100), and anatase-(101) surfaces at room temperature (300 K). It was observed that anatase-(101) exhibits the longest-lived hydrogen bonds in terms of overall persistence, followed closely by rutile-(110). The relaxation times, defined as the integral of the autocorrelation of the hydrogen bond persistence function, were also larger for these two cases, while decay of autocorrelation function was slower. The increased number and overall persistence of hydrogen bonds in the adsorbed water monolayers at these surfaces, particularly for anatase-(101), may serve to promote possible water photolysis activity thereon.

[a)] Corresponding author. Tel: +35317161646. Email: niall.english@ucd.ie

Introduction

Since Fujishima and Honda observed that TiO_2 could split water under visible-light irradiation to produce hydrogen and oxygen gases [1], the study of properties of aqueous solutions in contact with TiO_2 interfaces has become a subject of considerable activity. There are many potential renewable energy applications in photo-electrochemical water splitting or dye-sensitised solar cells, not only for TiO_2, but for a range of semiconductor-water interfaces, often exploiting support-metal-support-interaction (SMSI) modification of photo-catalytic properties [2]. Although TiO_2 is one of the most studied metal oxides in the literature, there is somewhat limited understanding of interfacial water molecules' behaviour and reactivity at interfaces, despite recent progress in this area [3, 4], including by theoretical and molecular simulation methods [5]. Such interfaces provide a rich environment for investigation of confinement of water molecules' motion; this is particularly true where hydrogen-bonded molecules play an important role in stabilising solutes via solvent interactions and forming "cages" [3, 4]. Indeed, experimental vibrational spectra of adsorbed water on both rutile rods and anatase powder have been reported via inelastic neutron scattering (INS) measurements, concluding that the confined adsorbed water molecules exhibit vibrational and dynamical features closer to less mobile ice vis-à-vis the liquid [6, 7]. Molecular dynamics (MD) has been useful in characterising to some extent the dynamical and vibrational behavior of water molecules adsorbed on rutile-(110) and anatase-(101) surfaces [8, 9]; *ab initio* MD (AIMD) has offered key insights into the librational motion of higher-frequency modes of water adsorbed to titania in very interesting recent studies [9, 10], but the somewhat restrictive computational limits on AIMD simulation duration makes it difficult to ascertain lower-frequency translational modes for a desired level of accuracy. Recently, we have carried out longer classical MD simulations to study, at least qualitatively,

intramolecular strain in confined, adsorbed water molecules at various titania surfaces, in addition to orientations of the water dipoles with respect to the surface normal [11], as well as to reproduce vibrational spectra results of confined monolayers at the surfaces in reasonable agreement with INS spectra [12]. In all of these abovementioned experimental and simulation studies of relatively confined water monolayers, hydrogen bonding with the bridging oxygen atoms at the titania surfaces has been remarked as an influential factor in leading to this behaviour distinct from bulk liquid water.

In order to scrutinise directly hydrogen bonding behaviour between absorbed water monolayers and bridging oxygen (Ob) atoms at the titania interface, and to evaluate their relative importance in determining the loss of liquid-like behaviour, in this study, we investigate dynamical properties of hydrogen bonds between adsorbed water molecules and a variety of rutile and anatase interfaces by means of analysis from equilibrium classical MD simulations. We have computed lifetimes (persistence times) of individual water-Ob hydrogen bonds, as well as autocorrelation functions (ACFs) of persistence functions to study their decay, and evaluated probability distributions of overall proportion of simulation time for which particular water-Ob hydrogen bonds were present (given that certain hydrogen bonds would be 'broken' but subsequently reform). This presents a detailed picture of hydrogen bond dynamical properties between the titania and water, showing the important contribution of these hydrogen bonds in influencing properties of the water monolayer.

Simulation Methodology

As described in our previous MD studies of titania-water interfaces [11, 12], all surfaces were cut from bulk rutile with lattice vectors $a_0 = b_0 = 4.593$ Å, $c_0 = 2.959$ Å (symmetry group

P42/MNM) and bulk anatase with lattice vectors $a_0 = b_0 = 3.776$ Å and $c_0 = 9.486$ Å (symmetry group *I41/AMD*). The stability of the surfaces are in the decreasing order 110 > 100 > 101 for rutile [13]. Rutile-(110) and anatase-(101) are the most stable and studied surfaces, for which considerable experimental data are available. The rutile-(110) surface was cut for charge compensation to yield a non-polar and dipole-free surface [3, 11]. Every titanium surface atom has some extent of under-saturation in its coordination. Although the rutile-(110) surface atoms have been assigned charges [14] for classical dynamics, we have not applied these in the MD of the present simulations so as to enable comparison between different surfaces, and for consistency with our earlier simulation studies [11, 12]. In addition, specific charges or force-field parameters for atoms on other surfaces are unavailable in the literature. Our previous simulation studies also show that charges for bulk rutile work reasonably well for all of the surfaces studied [11, 12]. Rutile-(101) has a natural slanting angle with respect to the [001]-direction (or the laboratory *z*-direction, *i.e.*, the direction of heterogeneity is orthogonal to the surface in the *x*-*y* plane, cf. Fig. 1a), which was corrected by aligning the entire slab orthogonal to the *z*-axis, so as to facilitate an orthorhombic periodic box. The surface of rutile-(001) is more acidic due to highly unsaturated four-coordinated Ti atoms [3, 4]. Anatase is the most photoactive polymorph of TiO_2 and is more stable at nanoscale dimensions than rutile [15], and hence is an important surface for this study; the anatase-(101) surface is also tilted at an angle and was aligned vis-à-vis the *z*-axis (cf. Fig. 1d). Since rutile-(001) and anatase-(001) are unstable, and therefore no neutron scattering data is available, they have been excluded from this study. The details of the system sizes and simulation box dimensions are specified in Table I.

[insert Table I and Figure 1 about here]

Reference to Fig. 1a shows that the rutile-(110) surface consists of bridging oxygen atoms bonded to 6-coordinated titania (Ti_{6c}), and a 3-coordinated oxygen (O_{3c}) bonded to Ti_{5c} and Ti_{6c} atoms. These Ti_{5c} surface atoms were used as the plane against which height measurements of water oxygen (O_w) atoms were made. Surface termination produces coordinatively unsaturated – sites (CUS), which differ in charge from the bulk. The rutile-(100) surface is shown in Fig. 1b, which constitutes about 20% of bulk rutile [3], and has a ridge pattern created by two-coordinated bridging oxygen atoms connected to Ti_{5c}. The rutile-(100) surface is similar to that of rutile-(110), except that the bridging plane of Ti_{5c}–O_b–Ti_{5c} is inclined at an angle, rather than perpendicular as in (110), *i.e.*, it has a sawtooth-like orientation. The rutile-(101) plane, depicted in Fig. 1c is similar to that of rutile-(100), and also composes 20% of naturally-occurring rutile [3]. It is also composed of Ti_{5c} and O_{2c} structures, but the Ti_{5c} bond length differs to the O_{2c}, creating two different types of O_{2c}. Also, the rutile-(101) plane is tilted with respect to the *z*-direction, and was rotated for alignment vis-à-vis the *z*-direction. It is also a non-planar structure. The anatase-(101) surface (cf. Fig. 1d), exhibits a terrace-like structure formed by fully-coordinated Ti_{6c} atoms bonded to O_{3c} atoms and under-coordinated Ti_{5c} with O_{2c}. The surface is tilted at an angle with respect to the [101] direction, and was rotated to align with the *z*-axis, *i.e.*, [001].

The force field used was as reported by Bandura *et.al*. [14] and Predota *et.al.* [16] for all surfaces, the flexible water model of which is summarised in Table II, together with cross interaction parameters; the Matsui-Akaogi force-field was applied to titania [17]. A flexible water model was employed in this study to be consistent with our previous simulations which studied intramolecular distortion [11] and vibrational and librational spectra [12] in the adsorbed water layers, and also because flexible models may be expected to offer, in general, at least as

much of a realistic description of water interactions with the surface, of central relevance for hydrogen bonding. The Ti-water oxygen (Ow) parameter was set to that of the titania Ti-O Buckingham potential and the Ow-oxide oxygen parameters were set to those of the SPC-Fw Lennard-Jones potential. The oxide surface was fully mobile throughout the simulations. Water molecules were added in the *z*-direction at the liquid density, as specified in Table I. The number of water molecules added was selected so that the bulk-like water density far from the surface (and its periodic image) was 1 g/cm^3. The Ewald method [18] was used to handle long-range electrostatics to within a relative precision of 10^{-5}, as implemented in the DL_POLY v2 package [19]. MD was performed using periodic boundary conditions in a Nosé-Hoover NVT ensemble with a relatively mild coupling period of 0.5 ps at 300 K using velocity-Verlet integration [18] with a 0.33 fs timestep, so as to sample adequately high-frequency vibrations of water molecules' oxygen-hydrogen (Ow-Hw) stretch modes. The whole system was equilibrated for up to 200 ps. Following this, production runs were carried out for 100 ps and snapshots sampled every 1 fs. Hydrogen bonds between waters' hydrogen atom donors and titania's bridging oxygen acceptors were identified by geometric criteria: a pair is considered to be hydrogen bonded if the oxygen-oxygen distance is less than 3.5 Å and the Ow-Hw⋯Ob angle is greater than 150°, with all Ow-Hw⋯Ob angles classified as being between 0 and 180° [20]. The relaxation of hydrogen bonds may then be characterised by an autocorrelation function $c(t)$ [21, 22]

$$c(t) = \langle h(0)h(t)\rangle / \langle h(0)h(0)\rangle \qquad (1)$$

where $h(t) = 1$ if a given pair is hydrogen bonded at time t, and $h(t) = 0$ otherwise. The ACF was evaluated for up to 50 ps, well past the persistence time of any individual hydrogen bond. In

addition, the duration, or persistence time, of each and every hydrogen bond was recorded and a probability distribution obtained, as well as recording the overall proportion of the simulation trajectory for which hydrogen bonds were extant between particular pairs of water protons and titania bridging oxygen atoms; this allows for distributions of individual and overall persistence to be gauged for each surface, ranging from sub-picosecond transient hydrogen bonds to substantially more long-lived ones. The integral of the (normalised) ACF in eqn. 1 serves to give an estimate of the overall relaxation time [21, 22], while comparison of the integral of un-normalised ACFs between different surfaces affords a relative comparison of overall water–titania hydrogen bonding relaxation times.

[insert Table II about here]

Results and Discussion

Normalised probability distributions of persistence times of each individual water - O_b hydrogen bond (*i.e.*, for lengths of consecutive times for which the persistence function $h(t) = 1$), are depicted in Fig. 2, for up to 0.2 ps; it generally decays after this, and this decay process shall be examined in some detail shortly. Although normalisation has been applied (such that the areas under the distributions, when extended out to long times, are unity, according to the appropriate definition of any probability distribution), it is readily apparent that many of the individual hydrogen bonds' lifetimes (or, more correctly, persistence times), are shorter at the rutile-(110) and anatase-(101) surfaces, with peaks in the region of 5-12 and 30-40 fs in both cases. It is interesting to note these two prominent peaks for the rutile-110 and anatase-101 surfaces, with three less distinct ones for the rutile-100 surfaces. This was found to arise from the anisotropy of

the vibrational modes of water molecules in the monolayer for the former two surfaces, in contrast to the relative isotropy of such modes in the latter case, with little difference in vibrational and librational modes in each direction [12]. Also, the more terraced-like structure of rutiles-(100) and –(101) (cf. Figs. 1 b & c) renders it more likely that individual hydrogen bonds can persist for slightly longer periods. However, the normalisation of the probability distribution is somewhat misleading, in that it does not take into account the overall greater number of water - O_b hydrogen bonds that are present at the rutile-(110) and anatase-(101) interfaces, *i.e.*, the significantly greater propensity for such hydrogen bonds to form at these surfaces. This was gauged by integration of the un-normalised ACF of eqn. 1 (which reflects the number of individual hydrogen bonds, as well as their persistence times), and the ratio was then taken vis-à-vis anatase-(101), which was found to exhibit the largest value; these are summarised in Table III as τ_{int} / $\tau_{int,\ a\text{-}101}$. The relaxation time from integration of the normalised ACF of anatase-(101) was found to be 0.085 ps, which is in excess of the shorter femtosecond timescales required for 'wet' electron transfer from water and aqueous solutions to titania surfaces in photo-excitation [3-5]. Rutile-(110) has almost the same relaxation time at 99% of the anatase-(101) value, with somewhat smaller values for the rutile-(100) and –(101) surfaces; this indicates that although individual water-O_b hydrogen bonds here are more likely to have longer persistence times due to a more terraced structure (cf. Figs. 1 b & c and Fig. 2), the less open terraced structure tends to reduce the relative number of such hydrogen bonds, as reflected by lower τ_{int} / $\tau_{int,\ a\text{-}101}$ ratios; although the individual hydrogen bonds may persist for somewhat longer, their fewer number would tend to reduce the probability of wet electron transfer arising from more intimate contact.

[insert Fig. 2 and Table III about here]

The normalised ACFs are depicted in Fig. 3. It was found that there was a three-stage negative exponential decay evident in all cases, *i.e.*, that $c(t)$ could be fit successfully as

$$c(t) = \sum_{i=1}^{3} A_i \exp\left(-t/\tau_i\right) \qquad (2)$$

These fits are shown in Fig. 3 along with the original ACF values, while the decay times τ_i are provided in Table III. The first, sub-picosecond, decay process (dubbed '1') is rapid in nature, while the second and third processes reflect the slower decay of medium- and longer-term picosecond-scale correlation of hydrogen bonding events. The longer-time ACFs captures more collective detail than shorter-time consideration of the distribution of individual lifetimes (as in Fig. 2), *i.e.*, on re-occurrence of the same hydrogen bond between a particular water proton and bridging oxygen which may break and subsequently re-form due to thermal vibrational fluctuations at the surface (examined in some detail in ref. 12). From inspection of Fig. 3, it is evident that the ultimate decay of rutile-110 and anatase-101 is slower; the long-term decay is reflected by the successive breakage-cum-reformation events of individual hydrogen bonds that is largely absent for the more terraced-like rutile-(100) and –(101) interfaces. In these cases, individual waters were observed to be 'terrace-trapped' for less than a few picoseconds and subsequently diffused away; hence, the dominant feature in the decay of Fig. 3 b & c is given by the medium-term $A_2 \exp\left(-t/\tau_2\right)$ contribution. In contrast, the longer-term $A_3 \exp\left(-t/\tau_3\right)$ feature is clearly more important for the rutile-(110) and anatase-(101) cases, and this is also reflected by their larger τ_3 values of 5.4 and 6.4 ps, respectively. In order to investigate further the longer-term nature of *overall*, as opposed to individual, persistence times suggested by the slower decay of rutile-(110) and anatase-(101) hydrogen bonding in Fig. 3, the normalised probability distributions of overall persistence times between specific proton-O_b pairs as a proportion of

overall simulation time are shown in Fig. 4. It is readily apparent that rutile-(110), and, in particular, anatase-(101), show evidence of considerable long-term stabilisation of particular hydrogen bonds in excess of about 97% of the trajectory (i.e., to the very right of Fig. 4), which are composed of breakage and re-formation events. Such hydrogen bond stabilisation helps to support the view that these surfaces would allow the water molecules to be adsorbed in the appropriate position for sufficiently long to allow a greater extent of femtosecond-scale electron transfer [3-5] to occur. It is thus to be expected that the rutile-(110), and, in particular, anatase-(101) surfaces would lead to a greater extent of water photolysis, although this has not been investigated experimentally in any level of detail, to the knowledge of the authors.

[insert Figs. 3 and 4]

The observed relaxation, along with nature of the decay model in eqn. 2, is very different for bulk water at 298 K for the flexible water potential, for which there is a single decay time (process), with a relaxation time of circa 4.1 ps. This reflects the fact that in the bulk liquid each water molecule has around 3.8 hydrogen-bonded neighbours, on average, so that this greater number of hydrogen bonds vis-à-vis the case of water adsorbed to titania surfaces leads to stronger, much longer-lived hydrogen bonds in the case of bulk water.

It has been shown that vacancies at titania surfaces, expected experimentally, favour dissociation [23]. This would be expected to have an impact on the hydrogen bond dynamics, although it would be perhaps necessary to carry out *ab initio* MD studies of this to assess how any chemical adsorption would alter the hydrogen bond persistence and relaxation times in this situation. Also, it has observed that the presence of vacancies at titania surfaces may well be the most instrumental step in determining water photolysis [23], as opposed to the number, and

persistence, of hydrogen bonds at the surfaces; this would require *ab initio* simulations to clarify the nature of any chemical adsorption, as mentioned above. Such an investigation is beyond the scope of this article, in view of the significant challenges inherent in simulation length- and timescales.

As mentioned previously, the bulk charges [cf. Table II and Ref. 16] were applied to titania for the various surfaces, for consistency with previous simulation studies [11, 12], and because compatible surface-specific charges are unavailable for all of the surfaces but rutile-110 [14]. To assess any difference or similarity in the surface charge states, some calculations were repeated for rutile-110 using those of ref. 13, but the results obtained were broadly similar (agreeing to within 5-10 %); therefore, it is hoped that the use of bulk charges at the surface titania atoms is a reasonable approximation.

Conclusions

Equilibrium MD simulations have been performed to investigate the hydrogen bonding kinetics of water in contact with rutile-(110), rutile-(101), rutile-(100), and anatase-(101) surfaces at room temperature (300 K). Anatase-(101) exhibits the longest-lived hydrogen bonds in terms of overall persistence, followed closely by rutile-(110). The relaxation times, defined as integral of eqn. 1, when un-normalised , were also larger for these two cases at around 0.085 ps, while decay of autocorrelation function was slower also at 6.4 and 5.4 ps, respectively. The increased number and overall persistence of hydrogen bonds in the adsorbed water monolayers at these surfaces, particularly for anatase-(101) serves to suggest that this would lead to a greater extent of water photolysis, although it is difficult to make a definitive conclusion in this respect due to the contribution of vacancies to photolysis at rutile-water interfaces [23]. However, it must be

borne in mind that classical MD is limited to a study of physical adsorption, and therefore the application of *ab initio* MD (AIMD) methods would be a more desirable future direction to study hydrogen bonding at these surfaces, despite its shorter-time resolution, given that chemical adsorption is also a salient and relevant observed feature for some of these surfaces [3-5]. However, classical MD does afford a useful insight into the underlying features of hydrogen bonding between water and these surfaces, and has revealed the nature of hydrogen bond stabilisation at anatase-(101).

Acknowledgements

We acknowledge useful discussions with Christian Burnham and Damian Mooney. This material is based upon works supported by Science Foundation Ireland (SFI) under Grant No. [07/SRC/B1160]. We thank SFI and the Irish Centre for High-End Computing for the provision of high-performance computing facilities. The authors acknowledge the support of SSE Renewables.

References

(1) Fujishima, A.; Honda, K. *Nature* **1972**, *238*, 37.

(2) Haller, G.L.; Resasco, D.E., *Adv. Catalysis* **1989**, *36*, 173.

(3) Diebold, U. *Surf. Science Reports* **2003**, *48*, 53.

(4) Henderson, M.A., *Surf. Science Reports* **2002**, *46*, 1.

(5) Sun, C., et al., *J. Mater. Chem.* **2010**, *20*, 10319.

(6) Levchenko, A. A.; Kolesnikov, A. I.; Ross, N. L.; Boerio-Goates, J.; Woodfield, B. F.; Li, G.; Navrotsky, A. *J. Phys. Chem. A* **2007**, *111*, 12584.

(7) Spencer, E. C.; Levchenko, A. A.; Ross, N. L.; Kolesnikov, A. I.; Boerio-Goates, J.; Woodfield, B. F.; Navrotsky, A.; Li, G. *J. Phys. Chem. A* **2009**, *113*, 2796.

(8) Mattioli, G.; Filippone, F.; Caminiti, R.; Bonapasta, A. A. *J. Phys. Chem. C* **2008**, *112*, 13579.

(9) Kumar, N.; Neogi, S.; Kent, P. R. C.; Bandura, A. V.; Kubicki, J. D.; Wesolowski, D. J.; Cole, D.; Sofo, J. O. *J. Phys. Chem. C* **2009**, *113*, 13732.

(10) Russo, D.; Teixeira, J.; Kneller, L.; Copley, J. R. D.; Ollivier, J.; Perticaroli, S.; Pellegrini, E.; Gonzalez, M. A. *J. Amer. Chem. Soc.* **2011**, *133*, 4882.

(11) Kavathekar, R.; Dev, P.; English, N.J.; MacElroy, J.M.D. *Molec. Phys.* **2011**, *109*, 1649.

(12) Kavathekar, K; English, N.J.; MacElroy, J.M.D. *Molec Phys.* **2011**, *109*, 2645.

(13) Mendive, C.B.; Bredow, T.; Feldhoff, A.; Blesa, M.A.; Bahnemann, D. *Phys. Chem. Chem. Phys.* **2009**, *11*, 1794.

(14) Bandura, A. V.; Kubicki, J. D. *J. Phys. Chem. B* **2003**, *107*, 11072.

(15) Barnard, A. S.; Curtiss, L. A. *Nano Letters* **2005**, *5*, 1261.

(16) Predota, M.; Bandura, A. V.; Cummings, P. T.; Kubicki, J. D.; Wesolowski, D. J.; Chialvo, A. A.; Machesky, M. L. *J. Phys. Chem. B* **2004**, *108*, 12049.

(17) Matsui, M.; Akaogi, M. *Molec. Sim.* **1991**, *6*, 239.

(18) Allen, M. P.; Tildesley, D. J. *Computer simulation of liquids*; Oxford, 1987.

(19) W. Smith, M. L., T.R. Forester *The DL_POLY_2 User Manual*, v. 2.14 ed., Daresbury Lab., Great Britain, 2003.

(20) Luzar, A.; Chandler, D., *Phys. Rev. Lett.* **1996**, *76*, 928.

(21) Luzar, A.; Chandler, D., *Nature* **1996**, *379*, 55.

(22) Stillinger, F.H., 1975, *Adv. Chem. Phys.* **1975**, *31*, 1.

(23) Schaub, R.; Thostrup, P.; Lopez, N.; Lægsgaard, E.; Stensgaard, I.; Nørskov, J.K.; Besenbacher, F. *Phys. Rev. Lett.*, **2001**, *87*, 266104.

Surface, X, Y, Z (Å)		System Size
Rutile (110)	26.26, 45.47, 69.490	$(TiO_2)_{630}(H_2O)_{2000}$
Rutile (100)	22.97, 26.63, 70.00	$(TiO_2)_{405}(H_2O)_{950}$
Rutile (101)	27.33, 27.56, 113.47	$(TiO_2)_{300}(H_2O)_{2468}$
Anatase (101)	71.46, 26.43, 72.680	$(TiO_2)_{1176}(H_2O)_{3162}$

Table I: System sizes

Buckingham potential for TiO_2 and water oxygen : $A_{ij} \times exp(-r_{ij}/\rho_{ij}) - C_{ij}/r_{ij}^6$			
i – j	A_{ij}(kcal mol^{-1})	ρ_{ij}(Å)	C_{ij}(kcal mol^{-1} Å^6)
Ti – O	391049.1	0.194	290.331
Ti –Ti	717647.4	0.154	121.067
O – O	271716.3	0.234	696.888
Ti –Ow	28593.0	0.265	148.000
Lennard-Jones potential for water: $(q_iq_j/r_{ij}) + \varepsilon_{ij}[(\sigma_{ij}/r_{ij})^{12}-(\sigma_{ij}/r_{ij})^6]$			
i – j	ε_{ij} (kcal mol-1)	σ_{ij}(Å)	
Ow – Ow	0.1554	3.165492	
Harmonic potential for water: $k/2 \times (r_{ij}-r_0^2)$			
i – j	k_{ij} (Å^{-1})	r^0_{ij} (Å)	
$O_w – H_w$	1059.162	1.012	
Harmonic angle bending potential for water: $k/2 \times (\theta – \theta_0)$			
i – j – k	θ_0 deg	k (kcal mol^{-1}rad^{-2})	
H – O – H	113.24	75.900	
Atomic charges: q(Ti) = 2.196 *e*, q(O) = -1.098 *e*, q(O_w) = -0.82 *e*, q(H_w) = 0.41 *e*; O_w, H_w = water oxygen and hydrogen atoms			

Table II: Force-field parameters

Surface	τ_{int} / $\tau_{int,\ a\text{-}101}$	τ_1 (ps)	τ_2 (ps)	τ_3 (ps)
Rutile (110)	0.91	0.084 ± 0.0056	0.62 ± 0.17	5.4 ± 0.83
Rutile (100)	0.84	0.076 ± 0.0052	1.1 ± 0.28	2.5 ± 0.33
Rutile (101)	0.99	0.095 ± 0.0070	0.53 ± 0.12	4.3 ± 0.54
Anatase (101)	1	0.071 ± 0.0067	1.3 ± 0.35	6.4 ± 0.86

Table III: Overall integrated relaxation time with respect to that of anatase-101: this arises from the ratio of the integral of the un-normalised ACF of the persistence of water proton – O_b hydrogen bonds, the normalised ACFs of which are shown in Fig. 3, to the anatase-101 relaxation time from its normalised ACF, which is 0.085 ps. The fitted relaxation times τ_i for the normalised ACFs decay are also specified (in ps); cf. Fig. 3.

Figure Captions

Fig 1: Layout of various titania surfaces, as discussed in the text; the laboratory *z*-direction is vertical. Here, Ob denotes a bridging oxygen, O3c a three-coordinated surface oxygen, Ti5c a penta-coordinated surface Ti atom (a lone coordinatively unsaturated site), while Ti6c stands for a hexa-coordinated Ti atom. (a) rutile-110; (b) rutile-100 surface with the same surface elements as rutile-110, but tilted at an angle; (c) rutile-101; and (d) anatase-101.

Fig 2: Normalised probability distributions of each individual water - O_b hydrogen bond, shown for up to 0.2 ps only – it generally decays after that (with the exception of some longer hydrogen bonds – see Fig. 4).

Fig 3: ACF characterising relaxation of hydrogen bonds between water molecules and bridging oxygen atoms at various surfaces: (a) rutile-110; (b) rutile-100; (c) rutile-101, and (d) anatase-101. In all cases, the fitted exponential decay terms are shown.

Fig 4: Normalised probability distributions of overall percentage lifetimes of each set of hydrogen bonds between each distinct pair of water - O_b atoms. The various rutile surface results have been up-shifted by multiples of 0.05 for clarity of presentation.

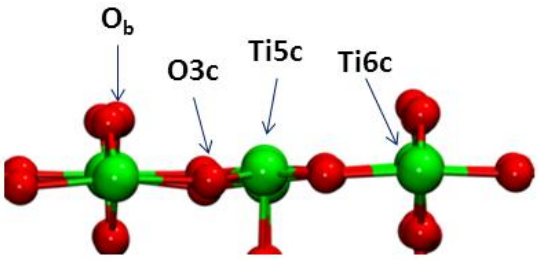

Fig. 1(a): Rutile-110

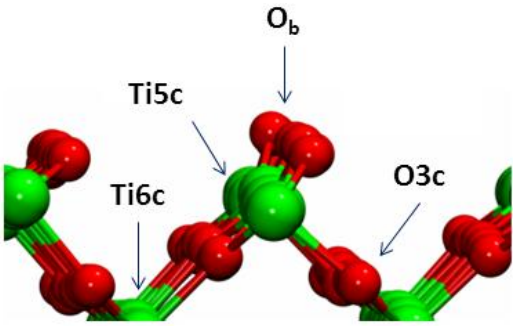

Fig.1(b): Rutile-100

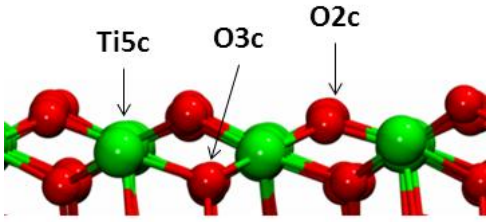

Fig. 1(c): Rutile-101.

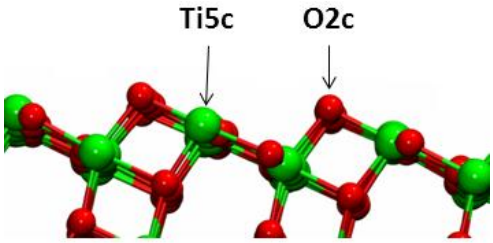

Fig. 1(d): Anatase-101.

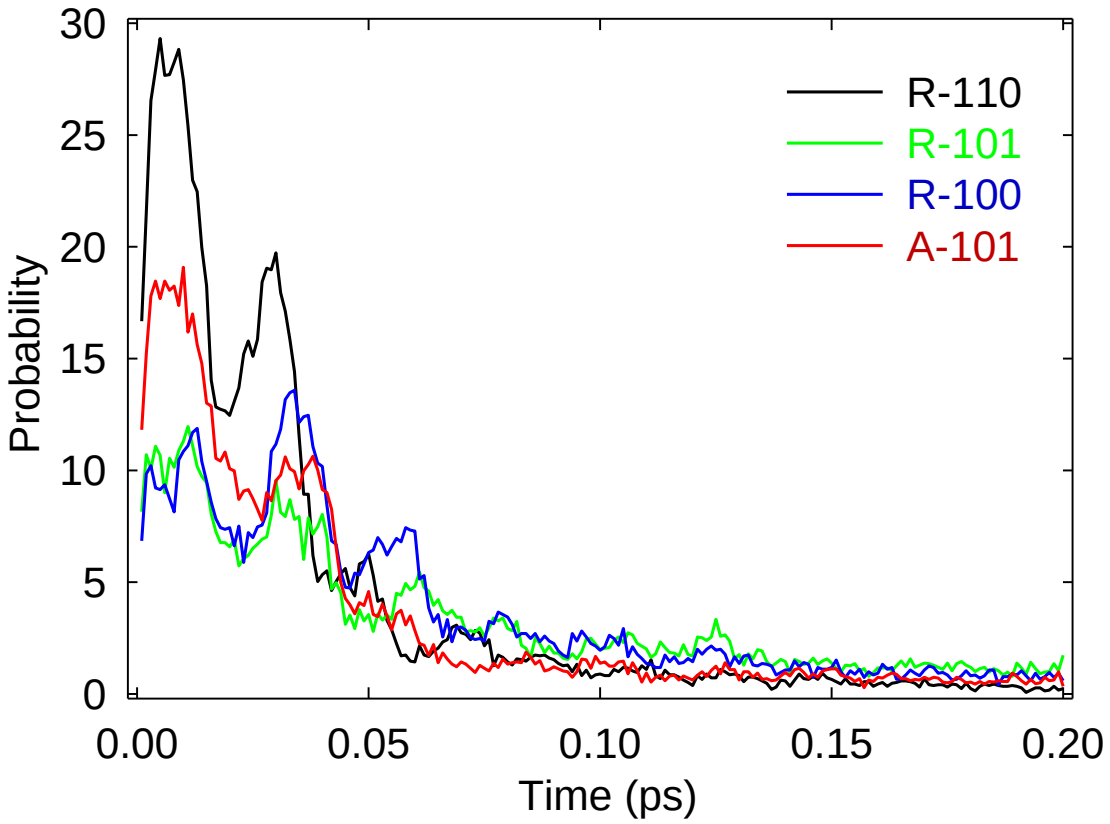
30
25
20
15
10
5
0
Probability
0.00
0.05
0.10
0.15
0.20
Time (ps)
R-110
R-101
R-100
A-101

Fig. 2

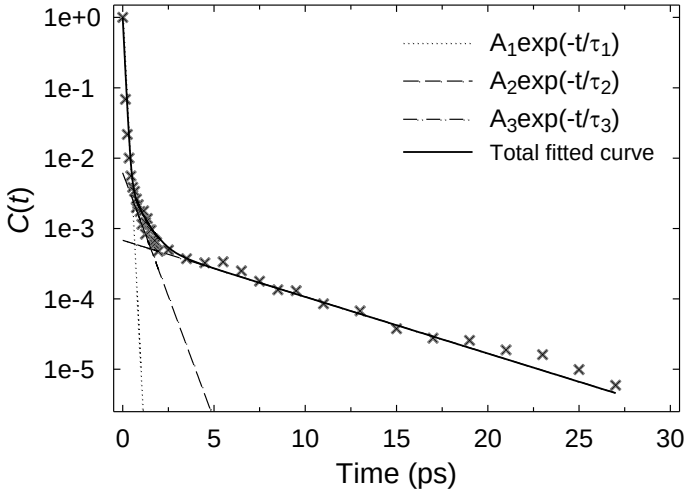

Fig. 3(a): Rutile-110

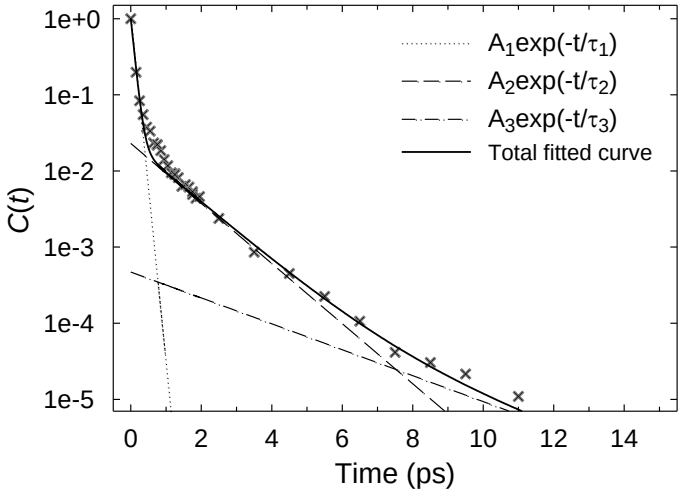

Fig. 3(b): Rutile-100

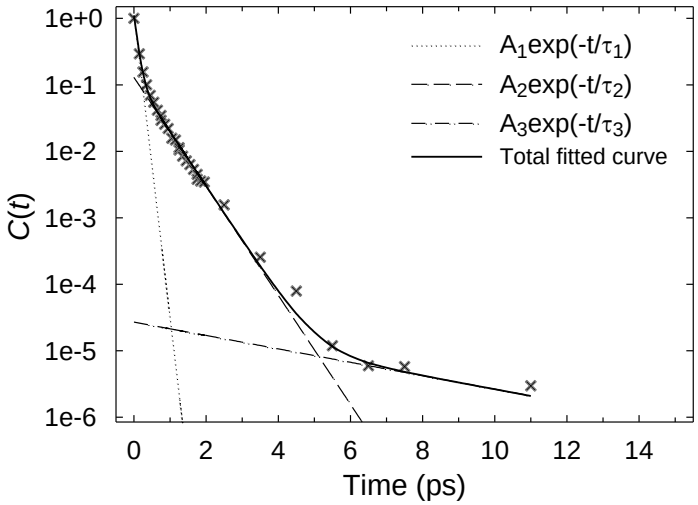

Fig. 3(c): Rutile-101

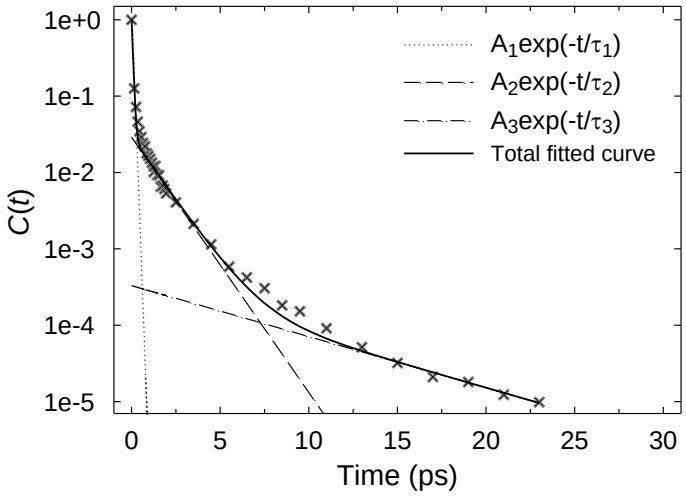

Fig. 3(d): Anatase-101

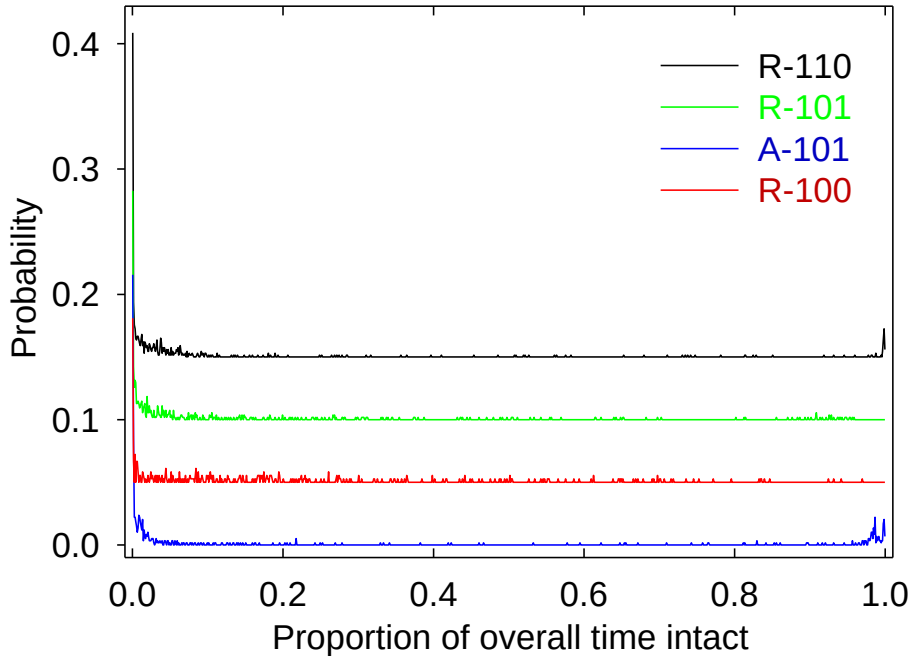
0.4
0.3
0.2
0.1
0.0
Probability
0.0
0.2
0.4
0.6
0.8
1.0
Proportion of overall time intact
R-110
R-101
A-101
R-100

Fig. 4